Advances in Engineering Science
Sect. C (3), July-September 2008, PP 61-66

IRIS RECOGNITION USING MULTI-DIRECTIONAL WAVELETS: A NOVEL APPROACH

R. M. Bodade[1]*, Dr. S. N. Talbar[2] and S. K. Ojha[3]

1 - Military College of Telecommunication Engineering, Mhow-45344, India
2 - SGGS Institute of Engineering and Technology, Nanded-431602, India
3 - Indian Army, India

ABSTRACT

The increasing requirement of security due to advances in information technologies, especially e-Commerce have led to rapid development of personnel identification /recognition systems based on biometrics. Iris is one of the most reliable biometrics because of its uniqueness, stability and non-invasive nature. A remarkable and important characteristic of the iris is the randomly distributed irregular texture details in all directions. In this paper, the authors have proposed a novel approach of feature extraction of iris image using a new method, 2D redundant rotated complex wavelet transform (RCWT) which obtains the features in 12 different directions, when used in conjunction with 2D Dual Trace Complex wavelet Transform(DT-CWT) against 3 and 6 directions in Discrete Wavelet Transform (DWT) and Complex Wavelet Transform (CWT) respectively. Iris features are obtained by computing 36 energies and 36 standard deviation of detailed coefficients in 12 directions per stage, at 3 level of decomposition. Canbera distance is used for matching. The results are obtained using DWT, CWT and combination of CWT and RCWT on UBIRIS database of 2400 images. The performance measure, ZeroFAR is reduced from 6.3 using DWT to 2.7 using the proposed method. The results are also comparable with the Daughman method. The method is also computationally efficient as compared to Gabor Filters.

Key words : *Iris Recognition; RCWT; CWT; Multi-directional wavelets; Biometrics.*

1. INTRODUCTION

The increasing requirement of security due to advances in information technologies, especially, e-Commerce have led to rapid development of personnel identification /recognition systems based on biometrics[1]. Iris is one of the most reliable biometrics because of its uniqueness, stability and non-invasive nature [2]. The human iris is an annular part between the pupil (black) and the white sclera as shown in figure (1-a). A remarkable and important characteristic of the iris is the randomly distributed irregular texture details in all directions[3]

Iris texture analysis using DWT provides singularities (edges) in only three directions *{0^0, 45^0, 90^0}* and without phase information which is improved by finding the singularities, with phase information, in 12 directions *{-15^0, -30^0, -45^0, -60^0, -75^0, 0^0, 15^0, 30^0, 45^0, 60^0, 75^0, 90^0}* and at many freq bands using 3 level RCWT in conjunction with CWT *to* achieve better accuracy and efficiency at less computational cost as compared to existing methods.

The remainder of this paper consists of existing iris recognition techniques, localization and normalization, novel feature extraction method, matching, experimental results and conclusions covered in Section-2, 3, 4, 5, 6 and 7 respectively.

2. EXISTING IRIS RECOGNITION TECHNIQUES

Major work on iris recognition[3-10] has been done in last 10-15 years. One of the most successful system proposed by Daugman[3] is based on phase band code using Gabor filters. Wildes et al. [5] has used a Laplacian pyramid at four levels; systems based on zero crossing representation of wavelets

*rajeshbodade@gmail.com

were proposed by W. Boles *et al.* [6] and C. Sanchez-Avila *et al.* [8]. R. Sanchez-Reillo *et al.* have used Gabor filters for feature extraction and a stastical matcher [7]. L. Ma *et al.* used texture analysis using Gabor filters in horizontal direction[9]. In [10] same authors used modified Gabor filters to capture iris information not only in horizontal direction[9] but also consider information from other directions to improve the results as compared to [5-9] but slightly inferior to [3].

Most of the methods stated used either one or other kind of wavelet transform for multiscale analysis or Gabor filter to find the features called iris code. However, there are well known limitations in the conventional wavelet design, for example the lack of directionality/phase information and poor shift invariance. Gabor filters are computationally less economical. These problems are addressed by CWT and further improved by the novel approach of combining RCWT and CWT while benefiting from the existing advantages that wavelets and Gabor provide.

3. IRIS LOCALISATION AND NORMALISATION

In general, the process of iris recognition can be described in three steps, viz., Localization and normalization of the iris, Feature Extraction and Matching. In this work, UBIRIS Database [11] is used for testing and result generation. It consists of 2400 images of 240 subjects and of 800x600 pixels resolution.

From the empirical study of the database, following parameters are found:

(a) Range of iris radii varies from 100 to 130 pixels.

(b) Range of pupil radii varies from 40 to 65 pixels.

(c) Upper and lower limits for iris and pupil centre are 140 and 100 pixels respectively.

Using the stated data, the outer boundary detection, the pupil detection and the normalization algorithms on gray scale eye image of iris, the rectangular iris image of 512x36 pixels is derived which is further enhanced by local filtering mask of 16x16 pixel. figure 1(a to e) shows the output at different steps in the process of Iris Localisation.

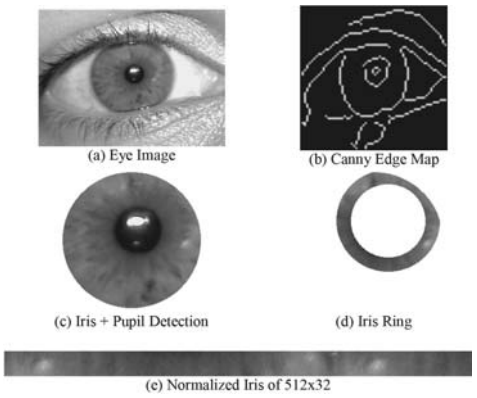

Figure 1 : Iris Localisation and Normalisation

In contrast with other methods, this method does not insist for the quality assessment of eye image and considers almost all images whose count is more than 128 out of 512 as valid iris image for detection. Thus, it creates more challenges for feature extraction method.

4. FEATURE EXTRACTION

4.1 Dual Tree Complex Wavelet Transform

In dual-tree, two real wavelet trees are used as shown in figure (2), each capable of perfect reconstruction (PR). One tree generates the real part of the transform and the other is used in generating complex part[12]. As shown, {H0 (z), H1 (z)} is a Quadrature Mirror Filter (QMF) pair in the real-coefficient analysis branch. For the complex part, {G0 (z), G1 (z)} is another QMF pair in the analysis branch.

All filter pairs are orthogonal and real-valued. It has been shown [13] that if filters in both trees be made to be offset by half-sample, two wavelets satisfy Hilbert transform pair condition and an approximately analytic wavelet is given by Eq(1).

$$\psi(x) = \psi_h(x) + j\psi_g(x) \qquad \text{-------Eq(1)}$$

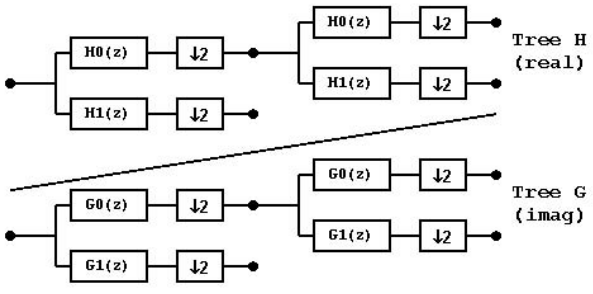

Figure 2 : Selesnick's Dual Tree DWT

Thus, if $G_0(\omega) \cong H_0(\omega) \times e^{-j\theta(\omega)}$ *and* $\theta(\omega) \cong \omega/2$

then $\psi_g(\omega) \cong -j\psi_h(\omega), \omega > 0$

$\cong j\psi_h(\omega), \omega < 0$ ---------- Eq(2)

From Eq(1) and (2), low pass filters after the first stage and at first stage respectively are given by Eq(3):

$g_0(n) = h_0(n\text{-}0.5)$ and $g_0(n) = h_0(n-1)$ -------Eq(3)

Similar relations also hold true for high pass filters.

In this algorithm, (10,10)-Tap near orthogonal wavelet filters are used in first stage and 'db7' filters are used for higher stages in the real tree (i.e. h_0 and h_1)[12].The imaginary low pass filter is derived from the above half sample delayed condition. The high pass filter is the quadrature-mirror filter of the low pass filter. The reconstruction filters are obtained by time reversal of decomposition filters. All the filters used are of same length based on Selesnick's approach [12][13][14] unlike Kingsbury's approach.

The 2D separable DWT can be written in terms of 1D scaling functions (φ) and wavelet functions (ψ) as:

$$\psi^{0}(x, y) = \phi(x)\psi(y)$$
$$\psi^{90}(x, y) = \psi(x)\phi(y)$$ ---------- Eq(4)
$$\psi^{\pm 45}(x, y) = \psi(x)\psi(y)$$

Oriented non-separable 2D wavelet transform is derived by combining the sub-bands of two separable 2D DWTs. The pair of conjugate filters are applied to two dimensions (x and y), which can be expressed by Eq(5) as given bellow:

$(h_x+jg_x)(h_y+jg_y)=(h_xh_y-g_xg_y)+j(h_xg_y+h_yg_x)$ -----Eq(5)

The filter bank structure of 2D DT CWT, to implement Eq(5) is shown in figure (3).

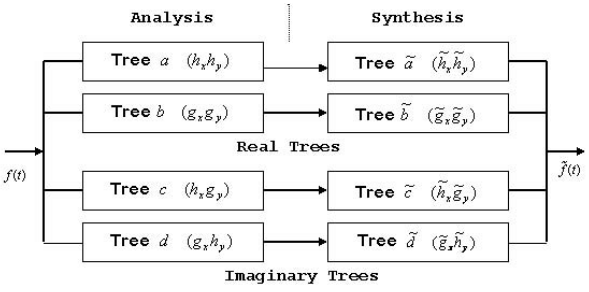

Figure 3 : Filter bank structure of 2D DT CWT

Tree-a and Tree-b are combined to compute the Real part of Eq(5) i.e. Real (2D DWT) tree of CWT as shown in figure (4). Similarly, Imaginary (2D DWT) tree of CWT can be obtained from Tree-c and Tree-d i.e. $(h_xg_y - g_xh_y)$, as per Eq(5).

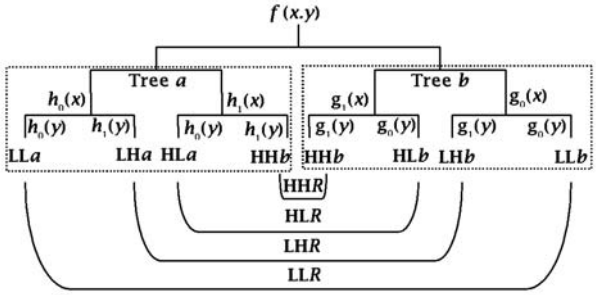

Figure 4 : Formation of Real Tree DT CWT

Thus, the decomposition for each mode is performed in a standalone mode, in one after another stage i.e. total of 6 detailed coefficients are derived at each stage; three for the real tree and three for the imaginary tree. 3-stage decomposition is performed. At each stage, coefficients are oriented towards their respective directions as stated in Eq(4). Following six wavelets, as given by Eq(6), are used to obtain oriented 2-D separable wavelets [12]:

$$\psi_{1,1}(x, y) = \phi_h(x)\psi_h(y), \quad \psi_{2,1}(x, y) = \phi_g(x)\psi_g(y),$$
$$\psi_{1,2}(x, y) = \psi_h(x)\phi_h(y), \quad \psi_{2,2}(x, y) = \psi_g(x)\phi_g(y),$$ Eq(6)
$$\psi_{1,3}(x, y) = \psi_h(x)\psi_h(y), \quad \psi_{2,3}(x, y) = \psi_g(x)\phi_g(y),$$

where, $\varnothing_{1,i}$ correspond to the coefficients derived from the real tree and $\varnothing_{2,i}$ correspond to the coefficients derived from the imaginary tree. They can be combined by Eq(7) to form complex wavelet coefficients.

$$\psi_i(x, y) = \frac{1}{\sqrt{2}}(\psi_{1,i}(x, y) - \psi_{2,i}(x, y)),$$
$$\psi_{i+3}(x, y) = \frac{1}{\sqrt{2}}(\psi_{1,i}(x, y) + \psi_{2,i}(x, y))$$ --------- Eq(7)

Normalization by $1/\sqrt{2}$ *is used so that the sum* difference operation constitutes an orthonormality. These six wavelet sub-bands of the 2-D DT-CWT are strongly oriented in {+15°,+45°,+75°, -15°, -45°, -75°} direction as shown in figure (5) by red lines and it captures image information in those directions.

Thus, in particular, 2D dual-tree wavelets are not only approximately analytic but also oriented[12].

4.2 Dual Tree Rotated Complex Wavelet Transform

RCWT is obtained by rotating non-separable wavelet filters obtained using CWT by 45° so that the decomposition is performed along the new direction, which are 45° apart from decomposition directions of CWT. The set of filters for RCWT[15] retains the orthogonality property because it satisfy the condition given by Eq(8):

$$\frac{1}{2\pi}\int_{-\infty}^{\infty} S_i(\omega)\,\overline{S_j(\omega)}\,d\omega = 0, (i \neq j) \qquad \text{-----Eq(8)}$$

where $S_i(w)$ is the Fourier transform of the 2-D filter.

Another easier and computationally more efficient technique which is used in this paper makes use of the sub-bands of DT CWT for the computation of respective RCWT coefficients. The oriented and approximate rotated (by 45^0) complex wavelet transform can be obtained by using the various sub-bands of DT CWT, without designing the new set of rotated filters as proposed in[15] because when the CWT is rotated by 45^0 by maintaining the condition of orthogonality, the components of RCWT, {-30°, 0°, 30°, 60°, 90°, 120°(-60°)}, are derived by approximation of CWT, considering the fact that six directions of CWT are derived from three directions of two DWTs by approximation as stated by Eq(4) and Eq(6), e.g. +/-15^0 are horizontal components of real and imaginary trees of DT CWT are considered as an approximation of horizontal component (0^0) of basic DWT, similarly vertical (+/-75^0) and diagonal (+/-45^0) of CWT are respectively vertical (90^0) and diagonal (+/-45^0) components of DWT as shown in figure (5).

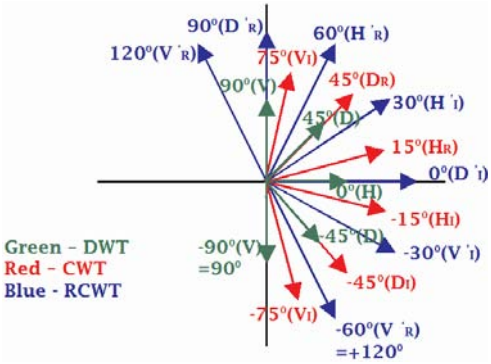

Figure 5 : Orientations of sub-bands of DWT, CWT and RCWT

The components of RCWT are {-30°, 0°, 30°, 60°, 90°, 120°(-60°)}, which are 45^0 rotated version of {-75^0, -45^0, -15^0, 15^0, 45^0, 75^0}. By close observation of figure (5), it is clear that, 0^0 (Imaginary diagonal component of RCWT) is close to -15^0 (Imaginary horizontal component of CWT) or 15^0 (Real horizontal component of CWT); we choose it -15^0 for uniform distribution of orientations. Thus, the diagonal component of imaginary tree of RCWT (0^0) is approximated as horizontal component of imaginary tree of CWT (-15^0).

The same approach is used to find the other components of RCWT from the various components of CWT.

Therefore, the sub-bands of RCWT in terms of horizontal, vertical and diagonal components of real and imaginary trees of CWT are obtained as given bellow:

1st subband = 1/v2(Real vert comp + Real diag comp)
2nd subband =1/v2(Real vert comp - Real diag comp)
3rd subband = 1/v2(Imaj vert comp + Imaj diag comp)
4th subband = 1/v2(Imag vert comp – Imaj diag comp)
5th subband = 1/v2(Real vert comp+ Imaj hori comp)
6th subband = 1/v2(Real vert comp - Imaj hori comp)

As these sub-bands are approximately 45^0 rotated versions of sub-bands of DT CWT, they are strongly oriented in {-30°, 0°, 30°, 60°, 90°, 120°(-60°)}, as shown in figure (7) by blue lines. Thus, by combining DT CWT and RCWT, the coefficients in 12 directions are computed by computing just four real 2D DWTs. Hence, the method is computationally economical as compared to Gabor filters used to compute the same. The energy and the standard deviation of 36 sub-bands(18 of CWT and 18 of RCWT, at 3 levels) of an iris is calculated using:

$$E_k = \frac{1}{M \times N}\sum_{i=1}^{M}\sum_{j=1}^{N}|W_k(i,j)| \qquad \text{-Eq(9)}$$

$$\sigma_k = \left[\frac{1}{M \times N}\sum_{i=i}^{N}\sum_{j=1}^{M}(W_k(i,j) - \mu_k)^2\right]^{\frac{1}{2}}$$

where W_k (i,j), (M X N) and μ_k are the k^{th} wavelet decomposed sub-bands, the size and mean value of wavelet decomposed subband respectively.

5. MATCHING

For better results, energy and standard deviation are combined to form a feature vector of 72 elements i.e.

$f_{óμ}$ = [ó1 ó2 …..ó36 E1 E2 …… E36]

Canberra distance metric as dissimilarity measure[15] is used which normalises the individual feature components before finding the distance between the two images. If x and y are the feature vectors of the database and query image, respectively and have dimension d, then the Canberra distance is given by Eq(10):

$$Canb\ (x, y) = \sum_{i=1}^{d} \frac{|x_i - y_i|}{|x_i| + |y_i|} \quad \text{---- Eq(10)}$$

6. EXPERIMENTAL RESULTS

The algorithms based on DWT, CWT, (RCWT+CWT) and Gabor Wavelet [Daughman] are implemented in MATLAB7.0 and executed on Intel PIV Mobile, 1.8 GHz, 789MHz, 256 MB RAM.

The proposed method is tested on UBIRIS database [11]. It consists of 2400 iris images of 240 subjects in two distinct sessions. For each database total 500 enrolment attempts are performed and a total of 1600 genuine matching attempts (template of each impression is matched against the remaining impression of same subject less symmetric match) and 3350 imposer matching attempts (template of the first impression with first impression of other subjects). These 34 irises are not correctly localized which means count is less than 128. The performance indicators adopted in this work are: ZeroFAR , processing time, length of feature set in bytes. Comparison of different methods is as shown in Table 1. Publicly available MATLAB library[16] is used for Gabor Wavelet (Daughman Method).

Table 1 : Average ZeroFAR, Average Processing Time (PT) and length of Feature Set in bytes (FS-B)

	DWT	CWT	RCWT +CWT	Gabor Wavelet
ZeroFAR(%)	6.3	4.1	2.7	2.6
PT(Seconds)	0.54 s	0.92	0.98	2.13
FS-B(Bytes)	72	152	304	256

A plot of FAR versus FRR as shown in figure (6) also confirms the benefit of the combination of CWT and RCWT method over the method using CWT only and certainly using DWT.

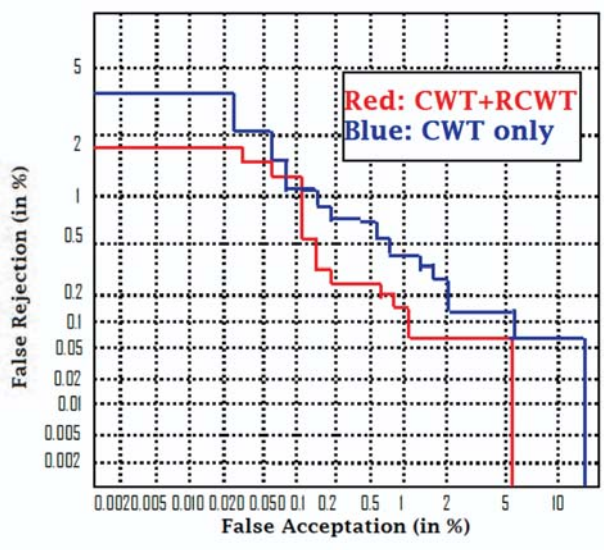

Figure 6 : FAR vs FRR plots of CWT and CWT+RCWT

7. CONCLUSIONS

The authors have introduced a new 2D DT RCWT derived from 2D DT CWT. According to randomly distributed irregular texture of iris, it is decomposed jointly with DT CWT and DT RCWT to capture orientation information in 12 different directions. The experimental results have demonstrated the effectiveness of the proposed method in terms of improving the recognition rate and processing time as compared to wavelet transform based methods and Gabor wavelet based methods respectively. Inherent shift invariance is the added advantage of this method[14].

The results can be improved further by adopting appropriate quality assessment scheme to reject bad quality image beforehand as proposed in[3][10]. In this work only 34 very bad images, whose count was less than 128 out of 512, were rejected.

8. REFERENCES

1. Biometrics: Personal Identification in a Networked Society, A. Jain, R. Bolle and S. Pankanti, eds. Kluwer,1999.
2. R. Johnson, “Can Iris Patterns Be Used to Identify People?” Chemical and Laser Sciences Division, LANL, Calif., 1991.
3. J. Daugman, “High Confidence Visual Recognition of Persons by a Test of Statistical Independence,” IEEE Trans. PAMI, vol. 15, no. 11, pp. 1148-1161, Nov. 1993.
4. J. Daugman, Biometric Personal Identification System Based on Iris Analysis, United States Patent, no. 5291560, 1994.
5. R. Wildes, “Iris Recognition: An Emerging Biometric Technology,” Proc. IEEE, vol. 85, pp. 1348-1363, 1997.
6. W. Boles and B. Boashash, “A Human Identification Technique Using Images of the Iris and Wavelet Transform,” IEEE Trans. Signal Processing, vol. 46, no. 4, pp. 1185-1188, 1998.
7. R. Sanchez-Reillo and C. Sanchez-Avila, “Iris Recognition With Low Template Size,” Proc. Int’l Conf. Audio and Video-Based Biometric Person Authentication, pp. 324-329, 2001.
8. C. Sanchez-Avila and R. Sanchez-Reillo, “Iris-Based Biometric Recognition Using Dyadic Wavelet Transform,” IEEE Aerospace and Electronic Systems Magazine, pp. 3-6, Oct. 2002.
9. L. Ma, Y. Wang, and T. Tan, “Iris Recognition Based on Multichannel Gabor Filtering,” Proc. Fifth Asian Conf. Computer Vision, vol. I, pp. 279-283, 2002.
10. L. Ma, Y. Wang, and T. Tan, “Personal Identification Based on Iris Texture Analysis,” IEEE Trans. On PAMI, vol. 25, No. 12, pp. 414-417, Dec 2003.
11. Hugo Proenc¸a and Lu´ýs A. Alexandre. UBIRIS: iris image database, 2004. http://iris.di.ubi.pt
12. Ivan W. Selesnick, Richard G. Baraniuk, and Nick G. Kingsbury, “The Dual Tree Complex Wavelet Transform: A Coherent Framework for Multiscale Signal and Image Processing”, IEEE Signal Processing Magazine, pp. 123-151, Nov05.
13. I.W. Selesnick, “The design of approximate Hilbert transform pairs of wavelet bases,” *IEEE Trans. Signal Processing*, vol. 50, no. 5, pp. 1144-1152, May 2002.
14. N.G. Kingsbury, “The dual-tree complex wavelet transform: A new technique for shift invariance and directional filters,” in Proc. 8th IEEE DSP Workshop, Utah, Aug. 9–12, 1998, paper no. 86.20.
15. M. Kokare, P.K. Biswas, and B.N. Chatterji, “Rotation invariant texture features using rotated complex wavelet for content based image retrieval,” in Proc. IEEE Int. Conf. Image Processing, Singapore, Oct. 2004, vol. 1, pp. 393-396.
16. Masek L, Kovesi P (2003), “MATLAB sourse code for a Biometric Identification System Based on Iris Paterns”, The school of Computer Science and Software Engineering, The University of Western Austrilia.

■